Hierarchical Morphologies Formed by ABC Star-Shaped Terpolymers

Kenichi Hayashida,[†] Noriyuki Saito,[‡] Shigeo Arai,[‡] Atsushi Takano,[†,§] Nobuo Tanaka,[⊥] and Yushu Matsushita*,[†]

Department of Applied Chemistry, Graduate School of Engineering, Nagoya University, Nagoya 464-8603, Japan; EcoTopia Science Institute, Nagoya University, Nagoya 464-8603, Japan; Precursory Research for Embryonic Science and Technology (PRESTO), Japan Science and Technology Agency, 4-1-8 Honcho, Kawaguchi 332-0012, Japan; and Center for Integrated Research in Science and Engineering, Nagoya University, Nagoya 464-8603, Japan

Received December 30, 2006; Revised Manuscript Received March 16, 2007

ABSTRACT: Three types of hierarchical morphologies, i.e., cylinders-in-lamella, lamellae-in-cylinder, and lamellae-in-sphere structures, have been identified for ABC star-shaped terpolymers by transmission electron microscopy and small-angle X-ray scattering. The samples are composed of polyisoprene (I), polystyrene (S), and poly(2-vinylpyridine) (P) whose volume ratios of I:S:P are 1.0:1.8:*X*, where *X* covers the range $4.3 \leq X \leq 53$. In the cylinders-in-lamella structures, cylinders of the component I in lamellar matrix of S are oriented perpendicular to the lamellar planes, resulting in aligning normal to the film surface, while alternating lamellae of the component I and S are stacked in cylinders along the directions of the cylindrical axes in the lamellae-in-cylinder structures.

Introduction

Structures containing multiple periodicities with different length scales and orientations, i.e., hierarchical structures, have been found in several synthetic polymer systems.[1−6] Muthukumar et al. demonstrated that liquid-crystalline diblock copolymers form hierarchical morphologies by combining nanophase separation of the block copolymers with much smaller length scale organizations of the liquid-crystalline moieties within the nanophase-separated domains.[1] The same kinds of structures were also reported by Ruokolainen et al. using an oligomeric amphiphile hydrogen-bonded to comb−coil diblock copolymers.[2−4] The hierarchical morphologies were varied systematically from lamellae-in-sphere to lamellae-in-cylinder and to lamellae-in-lamella structures depending on their volume fractions.[3] Multiblock polymer systems also exhibit hierarchical morphologies.[5−9] Masuda et al. have demonstrated experimentally that an undecablock terpolymer, i.e., PISISISISIP, where I, S, and P denote polyisoprene, polystyrene, and poly(2-vinylpyridine) blocks, adopts a regular lamellar structure with double periodicities.[6] Theoretical investigations of phase behaviors of specific multiblock copolymer melts have been conducted by ten Brinke and co-workers. At elevated temperatures, a diblock-like phase separation was found, whereas a doublely periodic lamellae-in-lamella structure appeared upon reducing the temperature.[9]

In addition to the block copolymer systems mentioned above, ABC star-shaped terpolymers where three different polymer components are connected at one junction point are candidates for forming hierarchically self-organizing structures because the geometrical restriction constrains the junction points to be aligned in a single dimension. In fact, interesting morphologies have been observed experimentally for ABC star polymers in micellar systems. Lodge and co-workers reported segmented wormlike micelles formed in water.[10,11] In these micelles, two hydrophobic components constituted alternating flat disks and hydrophilic chains were anchored around circles formed at the intersection of the disks.

ABC star-shaped terpolymers also adopt characteristic phase-separated structures in condensed states if the three component polymers are immiscible. Much attention has been focused recently on experimental[12−23] and theoretical[24−31] investigations of nanophase-separated structures for the ABC star-shaped terpolymers. We previously reported characteristic cylindrical structures of ISP star-shaped terpolymers composed of polyisoprene (I), polystyrene (S), and poly(2-vinylpyridine) (P) based on the results obtained by using transmission electron microscopy (TEM) and microbeam small-angle X-ray scattering (SAXS).[18,21−23] The cross sections of the cylindrical structures revealed periodic tiling patterns consisting of even-numbered polygons for two sample series: one was $I_{1.0}S_{1.0}P_X$ series, where the volume ratio of I:S:P is 1.0:1.0:*X* and *X* covered the range $0.7 \leq X \leq 1.9$,[18,21] and the other series was $I_{1.0}S_{1.8}P_X$ series, where the volume ratio of I:S:P is 1.0:1.8:*X* and *X* covered the range $0.8 \leq X \leq 2.9$.[23] However, hierarchical structures have not been identified within these composition ranges.

On the other hand, Gemma et al. have predicted several hierarchical structures by a Monte Carlo simulation method for ABC star polymers with the arm-length ratio of 1:1:*x*.[25] The shapes of domains formed by the components A and B in these hierarchical structures were transformed from a lamellar into a cylindrical and into a spherical domain with the increase of *x* in the range $3 \leq x \leq 25$. We have also demonstrated the morphological transition from a lamellae-in-lamella to a lamellae-in-cylinder structure in the $I_{1.0}S_{1.0}P_X$ series covered the range $3.0 \leq X \leq 10$.[32] In this study, the internal structures in the hierarchical morphologies are all lamellar structures because the components I and S in the ISP star polymers have the same volume ratios. In present work, four ISP star-shaped terpolymers with asymmetric volumes for I and S components were synthesized whose volume ratios of I:S:P are 1.0:1.8:*X*, where *X* covers the range $4.3 \leq X \leq 22$, and the asymmetric effects

* To whom all correspondence should be addressed: e-mail yushu@apchem.nagoya-u.ac.jp; Tel +81-52-789-4604; Fax +81-52-789-3210.
[†] Graduate School of Engineering, Nagoya University.
[‡] EcoTopia Science Institute, Nagoya University.
[§] PRESTO, Japan Science and Technology Agency.
[⊥] Center for Integrated Research in Science and Engineering, Nagoya University.

10.1021/ma062972i CCC: $37.00
Published on Web 04/17/2007

Table 1. Characteristics of the ISP Star-Shaped Terpolymers

sample	M_n (10^3)	M_w/M_n [b]	$\Phi_I:\Phi_S:\Phi_P$ [d]
I	13.3[a]	1.04	−
S	27.4[b]	1.01	−
$I_{1.0}$-*b*-$S_{1.8}$	40.7[c]	1.03	1:1.82:0
$I_{1.0}S_{1.8}P_{4.3}$	110[c]	1.01	1:1.8:4.3
$I_{1.0}S_{1.8}P_{6.4}$	147[c]	1.02	1:1.8:6.4
$I_{1.0}S_{1.8}P_{12}$	241[c]	1.03	1:1.8:12.2
$I_{1.0}S_{1.8}P_{22}$	401[c]	1.04	1:1.8:22.0

[a] Determined by ^{1}H NMR. [b] Determined by SEC using polystyrene standard samples. [c] Estimated by ^{1}H NMR based on M_n of the S precursor. [d] Volume ratios of I:S:P calculated using bulk densities of the components, i.e., 0.926, 1.05, and 1.14 g/cm^3 for the I, S, and P components, respectively.

Table 2. Blend Ratios of the ISP Star-Shaped Terpolymers and hP To Obtain the $I_{1.0}S_{1.8}P_X$ Series

sample	formulation	weight fraction	$\Phi_I:\Phi_S:\Phi_P$[a]
$I_{1.0}S_{1.8}P_{9.6}$	$I_{1.0}S_{1.8}P_{6.4}/I_{1.0}S_{1.8}P_{12}$	0.35/0.65	1:1.8:9.6
$I_{1.0}S_{1.8}P_{11}$	$I_{1.0}S_{1.8}P_{6.4}/I_{1.0}S_{1.8}P_{12}$	0.16/0.84	1:1.8:11
$I_{1.0}S_{1.8}P_{32}$	$I_{1.0}S_{1.8}P_{22}$/hP	0.70/0.30	1:1.8:32
$I_{1.0}S_{1.8}P_{53}$	$I_{1.0}S_{1.8}P_{22}$/hP	0.44/0.56	1:1.8:53

[a] Volume ratios of I:S:P calculated using bulk densities of the components, i.e., 0.926, 1.05, and 1.14 g/cm^3 for the I, S, and P components, respectively.

on their hierarchical morphologies were investigated by transmission electron microscopy (TEM) and small-angle X-ray scattering (SAXS).

Experimental Section

Sample Preparations. Star-shaped polymer samples composed of polyisoprene (I), polystyrene (S), and poly(2-vinylpyridine) (P) were synthesized by anionic polymerizations as reported previously.[23] Table 1 summarizes the volume ratios of the three components in the four ISP star-shaped terpolymers prepared in this study together with their molecular weights and molecular weight distributions (MWDs). The compositions were determined using a 500 MHz ^{1}H NMR spectrometer (Varian Inc., Unity Inova 500). The number-average molecular weight of the common polystyrene and the MWDs of all the polymer samples were determined by SEC using standard polystyrene samples. The analyses were carried out using a SEC system (Tosoh Ltd.) equipped with a set of three separation columns of 300 mm × 7.8 mm i.d.—$G4000_{HR}$ for $I_{1.0}S_{1.8}P_{4.3}$ and $I_{1.0}S_{1.8}P_{6.4}$ and $G5000_{HR}$ for $I_{1.0}S_{1.8}P_{12}$ and $I_{1.0}S_{1.8}P_{22}$—and a refractive index detector (RI-8021). Several other samples were also obtained by blending two star polymers or by blending homopolymers with the sample $I_{1.0}S_{1.8}P_{22}$, as shown in Table 2. The samples with X of 9.6 and 11 were prepared by blending the two parent samples, $I_{1.0}S_{1.8}P_{6.4}$ and $I_{1.0}S_{1.8}P_{12}$, while two other polymer samples with X of 32 and 53 were prepared by blending $I_{1.0}S_{1.8}P_{22}$ and a low molecular weight poly(2-vinylpyridine) (M_n = 10K).

Morphological Observations. Sample films were obtained by solvent-casting from 5% solutions of the samples in THF for 2 days in most of the experiments. Exceptionally, 1,4-dioxane and toluene were also used to check casting solvent effects on morphology for the sample $I_{1.0}S_{1.8}P_{6.4}$. 1,4-Dioxane is a poor solvent for polyisoprene and a good solvent for poly(2-vinylpyridine), while toluene is a poor solvent for poly(2-vinylpyridine) and a good solvent for polyisoprene and polystyrene. The films were dried at room temperature for 12 h and annealed at 170 °C under a vacuum for 3 days except as-cast sample films for the solvent effect experiments. For TEM observations, the samples were cut into ultrathin sections having a thickness range of 25−75 nm using an ultramicrotome (Reica, Ultracut FCS) with a diamond knife (Diatome, cryo T) at room temperature. The sections were successively stained with osmium tetroxide and iodine. Osmium tetroxide stains component I heavily while iodine stains component P intermediately. The stained films were observed on a transmission electron microscope (Hitachi, H-800) operated at an accelerating voltage of 100 kV.

SAXS measurements were performed using the beamline 15A at Photon Factory (Tsukuba, Japan). The wavelength of the X-ray was 0.154 nm, and the size of the X-ray beam was ca. 0.4 mm × 0.7 mm (fwhm). The precise camera length was calibrated to be 2.39 m with a collagen standard sample.

Results

Cylinders-in-Lamella Morphology. A hierarchical morphology was identified in a relatively lower X region, $4.3 \leq X \leq 11$. Figure 1a−c shows TEM images representing the hierarchical structure for the sample $I_{1.0}S_{1.8}P_{6.4}$ taken at the same sample location with different tilt angles. Since the samples were stained with osmium tetroxide and iodine for the TEM observations, black, white, and gray domains correspond to I, S, and P components, respectively. Figure 1a illustrates that I and S domains form layers together, and they constitute an alternating lamellar structure with layers of P domains. The TEM images taken with tilt angles of 25° and 35° by inclining the sample around a horizontal axis (Figure 1b,c), reveal that the one combined layer made of the I and S components consists of cylindrical I domains in matrix of S. These TEM results suggest that the disklike cylindrical domains are aligned on the lamellar plane where the cylindrical axes are oriented perpendicular to the plane. Thus, the hierarchical cylinders-in-lamella morphology has been identified as schematically shown in Figure 1d.

The orientation of the hierarchical morphology to the sample film was determined by SAXS measurements. Figure 2a shows the two-dimensional SAXS pattern of the sample $I_{1.0}S_{1.8}P_{4.3}$ with the incident beam parallel to the film surface (edge view). Since the sample film was set horizontally for this measurement, the *z*-axis in the two-dimensional SAXS pattern is perpendicular to the film surface. The meridional scattering arcs give the lamellar *d*-spacing of 48 nm, while weak scatterings resulting from the internal cylindrical structure are also found on the equator in the same SAXS pattern. In Figure 2b, the two-dimensional SAXS pattern obtained from through view measurement is shown, where the incident X-ray was perpendicular to the film surface. Isotropic scatterings originating from the internal cylindrical structure as well as the lamellar structure are observed owing to random orientation. To separate the scatterings from the two structures, circularly averaged intensities for the two views are compared in parts a and b of Figure 3 for $I_{1.0}S_{1.8}P_{4.3}$ and $I_{1.0}S_{1.8}P_{6.4}$, respectively. Comparing the upper curves for the edge view and the lower ones for the through view, we notice three peaks each on the lower curves marked as 1′, 2′, and $\sqrt{7}'$ which clearly represent a hexagonal packing of the cylindrical domains. The magnitudes of the 1′ peak scattering vectors for $I_{1.0}S_{1.8}P_{4.3}$ and $I_{1.0}S_{1.8}P_{6.4}$, i.e., 0.219 and 0.201 nm^{-1}, give 29 and 31 nm for the $d_{\{10\}}'$-spacing, respectively, which are in good agreement with the values estimated from the corresponding TEM images. It should be noted that, in these scattering profiles for through view, $\sqrt{3}'$ peaks corresponding to {11} reflections for the internal cylindrical structures are almost invisible. This is due to the destructive interference resulting from the form factor for the cylindrical structure, where the volume fraction of the component I is about 0.35.[33] These SAXS results clarify that the lamellar structure is dominantly oriented parallel to the film surface, and consequently the cylindrical domains are oriented perpendicular to the film surface.

The morphologies mentioned above are observed for the sample films by casting from THF followed by annealing. However, it is well-known that morphologies of block copoly-

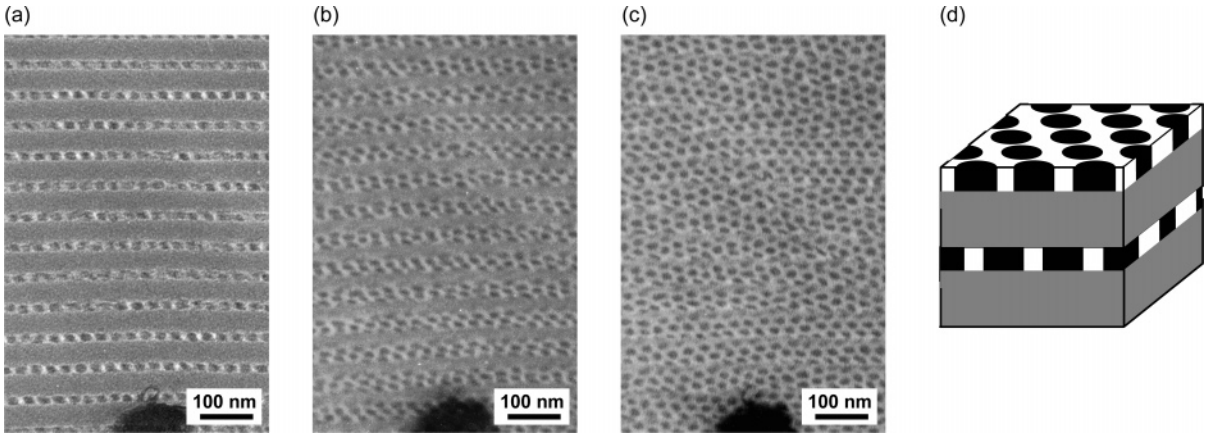

Figure 1. TEM images of a morphology for the sample $I_{1.0}S_{1.8}P_{6.4}$ taken with tilt angles of 0° (a), 25° (b), and 35° (c) around a horizontal axis at the same sample location and the corresponding schematic (d).

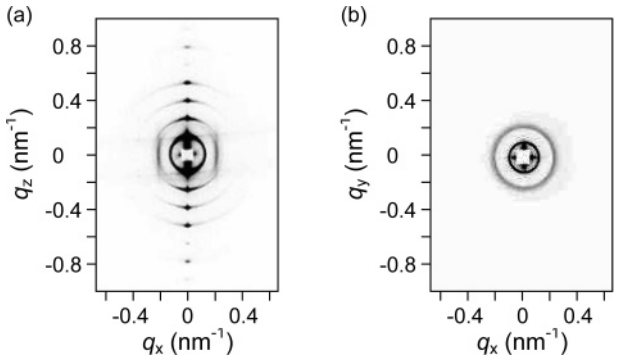

Figure 2. 2-Dimensional pattern SAXS patterns of $I_{1.0}S_{1.8}P_{4.3}$ with edge view (a) and through view (b).

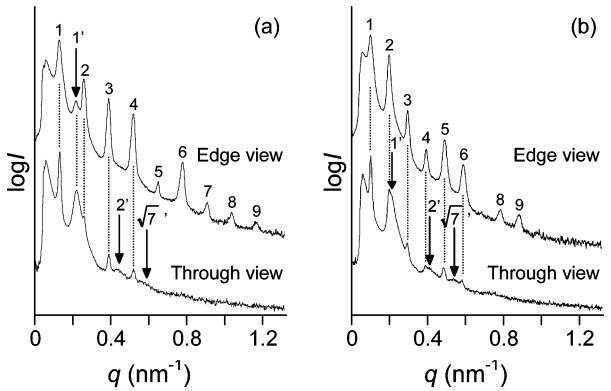

Figure 3. Circularly averaged SAXS profiles with edge and through views: (a) $I_{1.0}S_{1.8}P_{4.3}$ and (b) $I_{1.0}S_{1.8}P_{6.4}$.

mers are considerably affected by casting solvents. Figure 4 compares TEM images of as-cast films for $I_{1.0}S_{1.8}P_{6.4}$ from THF (a), 1,4-dioxane (b), and toluene (c), while Figure 4d was for the annealed film obtained by casting from toluene. Figure 4a exhibits a cylinders-in-lamella morphology for an as-cast film from THF which is the same as that for the annealed film shown in Figure 1. On the other hand, the structure observed for the as-cast film from 1,4-dioxane in Figure 4b is a lamellae-in-cylinder structure, while that from toluene is a cylindrical structure whose cross section reveals a new periodic tiling pattern, as shown in Figure 4c. However, both the structures were transformed into cylinders-in-lamella morphologies by annealing as shown in Figure 4d as an example.

Lamellae-in-Cylinder Morphology. Another hierarchical morphology was observed for the samples with X being in the range $12 \leq X \leq 32$. This lamellae-in-cylinder structure is essentially the same one as reported in previous works.[3,12,25,32] Figure 5a−c shows the TEM images of a lamellae-in-cylinder structure for the sample $I_{1.0}S_{1.8}P_{22}$ taken at the same sample location with three different tilt angles as in the case of Figure 1. These TEM images demonstrate that both I and S domains are shaped into disks individually, and they are alternately stacked, forming cylinders. Although an exact packing manner of these cylinders has not been identified at present, it seems to be a hexagonal one as schematically shown in Figure 5d according to Figure 5a. Furthermore, the arrangement of the cylinders has been predicted to be hexagonal by a simulation.[25]

Lamellae-in-Sphere Morphology. When X equals 53, sphere-like domains made of component I and S were observed. Figure 6a shows side views of the spheres in a TEM image of $I_{1.0}S_{1.8}P_{53}$. A single domain of the component I is sandwiched between two hemispheres of the S domains, forming a prolate sphere. This structure can be regarded as a lamellae-in-sphere morphology, as schematically shown in Figure 6b.

Discussion

As mentioned above, the three types of hierarchical structures have been observed for the ISP star-shaped terpolymers, i.e., cylinders-in-lamella, lamellae-in-cylinder, and lamellae-in-sphere morphologies. We notice that the junction points are aligned circularly for all the structures, and these results evidently come from the molecular design of the present samples. Several kinds of structure-in-structures have been observed for polymeric systems such as liquid-crystalline diblock copolymers,[1] comb−coil diblock copolymers,[2−4] multiblock copolymers,[5,6] and ABC star polymers.[32] The smaller length-scale organizations in these hierarchical morphologies have been limited to lamellar structures in all the previous works while cylinders-in-lamella structures found in this work have internal cylindrical structures with the shorter periodicities. The cylinders-in-lamella structures observed for $I_{1.0}S_{1.8}P_X$ ($4.3 \leq X \leq 12$) result from the asymmetric volume ratio of the component I and S, which enables the cylindrical domains of the I component in the matrix of the S component. Furthermore, it should be noted that the cylinders are oriented perpendicular to the lamellar planes in this new morphology, resulting in aligning normal to the film surface. This kind of vertical orientation of the cylindrical nanodomains to the film surface has scarcely been observed in bulk block copolymer systems. In the present ISP star system, however, the vertically oriented cylindrical domains are realized, being assisted by the parallel orientation of the lamellar planes to the film surface.

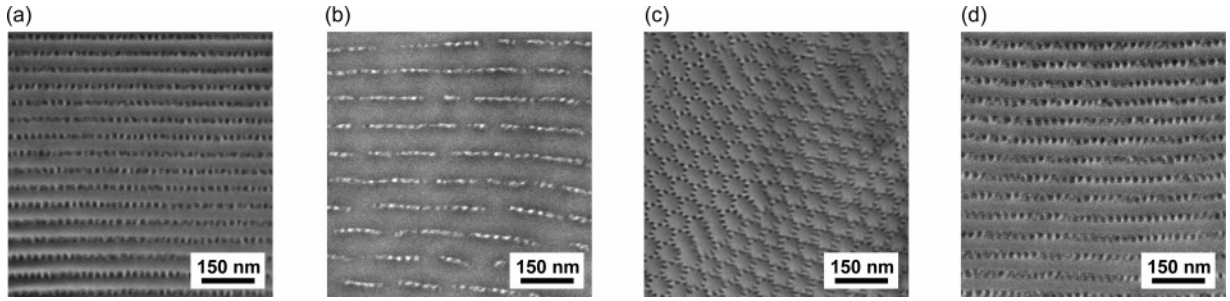

Figure 4. TEM images of morphologies for $I_{1.0}S_{1.8}P_{6.4}$ by casting from THF (a), 1,4-dioxane (b), and toluene (c, d) before (a−c) and after (d) annealing.

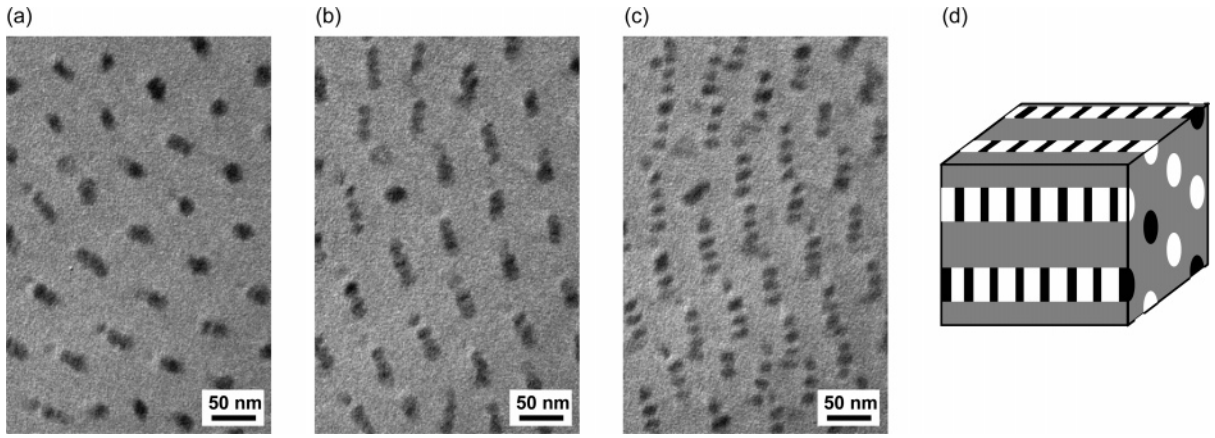

Figure 5. TEM images of a morphology for the sample $I_{1.0}S_{1.8}P_{22}$ taken with tilt angles of −20° (a), 5° (b), and 30° (c) at the same sample location and the corresponding schematic (d).

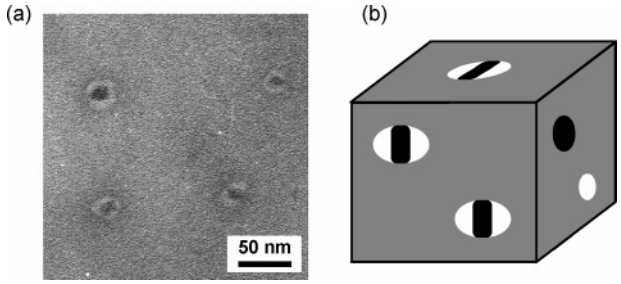

Figure 6. TEM image of the sample $I_{1.0}S_{1.8}P_{53}$ (a) and the corresponding schematic drawing (b).

This cylinders-in-lamella morphology is similar to hexagonal perforated layer (HPL) structures found in metastable states for diblock copolymers.[34−36] The stacking sequence of the hexagonal perforations in the HPL structure have been modeled as ABCABC and/or ABAB arrangements by two-dimensional diffraction patterns. On the other hand, in the SAXS pattern of the present cylinders-in-lamella morphology in Figure 2a, weak scatterings having the form of a vertical streak rather than a spot are found, resulting from the internal cylindrical structures. However, mutually correlated arrangements such as ABCABC or ABAB should give diffracted spots. The length of the streak is inversely related to the dimension of the scattering plane. Thus, the present result suggests that the stacking manner of the hexagonal layers are random in the cylinders-in-lamella structure, and hence the scatterings from the crystal plane as short as 19 nm in each independent layer are observed as the streaks.

By evaluation of the lamellar thickness in the cylinders-in-lamella morphologies for the three samples, $I_{1.0}S_{1.8}P_{4.3}$, $I_{1.0}S_{1.8}P_{6.4}$, and $I_{1.0}S_{1.8}P_{9.6}$, we notice an interesting fact. Table 3 compares the lamellar thicknesses of two lamellae for the P phase (D_P) and for the combined I and S phase (D_{I+S}) calculated by using

Table 3. Dimensions of the Cylinders-in-Lamella Morphologies for the $I_{1.0}S_{1.8}P_X$ Samples[a]

X	D_P (nm)	D_{I+S} (nm)
4.3	29.2	19.0
6.4	43.4	19.0
9.6	58.3	17.0

[a] D_{I+S} and D_P denote the lamellar thicknesses of the two lamellae for the P phase and for the I and S phase, respectively.

d-spacings obtained from SAXS measurements and the volume fractions of the samples. The thicknesses for the combined I and S phase are almost constant, especially when X equals 4.3 and 6.4. This finding means that the average distance of two junction points in the ISP star molecules does not change even if the P chain length increases. It is conceived that in a usual AB diblock copolymer system, lamellar thickness of the B domain decreases when lamellar thickness of the A domain increases with lengthening of the A chain because the average distance between junction points becomes longer due to the counterbalanced effects between interfacial energies and chain deformation energies. However, it is indicated that requirement for minimizing interfacial energy dominantly determines the lamellar thickness when X is in the range $4.3 \leq X \leq 6.4$ in the ISP star polymer system, for an increase of the average distance between the junction points causes an increase of the interfacial area for the components I and S against the component P. This interesting feature for the phase separation of ABC star polymers is attributed to high interfacial energy due to the lack of the junction points at the polymer−polymer interface for the systems.

Table 4 summarizes the morphologies formed by the $I_{1.0}S_{1.8}P_X$ star-shaped terpolymers. Shapes of domains formed by combined I and S phases are varied from matrix to lamellae, to cylinders, and to spheres, while those of P domains are varied from cylinders to lamellae and to matrix with increasing X.

Table 4. Morphological Transition for the $I_{1.0}S_{1.8}P_X$ Star-Shaped Terpolymers

X	morphology	combined I and S components	P component	Φ_P[b]
0	cylinder			0
0.8−2.9	cylinder[a]	matrix	cylinder	0.22−0.51
4.3−11	cylinders-in-lamella	lamella	lamella	0.60−0.80
12−32	lamellae-in-cylinder	cylinder	matrix	0.81−0.92
53	spherelike	sphere	matrix	0.95

[a] Cylinder-based structures whose cross sections give periodic tiling patterns identified in the previously work for the same $I_{1.0}S_{1.8}P_X$ star-shaped terpolymer series. [b] Volume fraction of the P component.

Although this morphological transition is analogous to that of $I_{1.0}S_{1.0}P_X$ star-shaped terpolymers,[32] the cylinders-in-lamella structure has been discovered instead of the lamellae-in-lamella structure because of the difference in the volume ratio of the I and S components. These morphological transitions of the two ISP star-shaped terpolymer series take place in essentially the same manner as those of a typical AB diblock copolymers. However, the composition range of the variable component P, at which each stable morphology is observed, is quite different from that for the AB diblock copolymers. In fact, the lamellar structure is exhibited up to 0.80 of the P volume fraction, which can be explained using the idea of an architecture effect known for A_2B star polymers.[12,37,38]

The morphology formed by the sample $I_{1.0}S_{1.8}P_{6.4}$ was strongly affected by casting solvents as shown in Figure 4. 1,4-Dioxane and toluene are poor solvents for polyisoprene and poly(2-vinylpyridine), respectively. Furthermore, the solubility of polystyrene in 1,4-dioxane is lower than those in THF and toluene.[39] Hence, the effective volume fraction of "the P phase" increases in 1,4-dioxane because the I and S shrink, which resulted in forming a lamellae-in-cylinder structure. On the other hand, the component P shrinks in toluene and forms cylindrical domains in a concentrated state. The cylindrical structures have been observed in the range of $0.8 \leq X \leq 2.9$ in our previous work.[23] However, the structure with the P domains surrounded by as many as 20 I and S cylindrical domains, as shown in Figure 6c, have never been observed before. It was confirmed that the morphologies formed from 1,4-dioxane and toluene are not stable ones because both structures were transformed into cylinders-in-lamella structures by annealing at 170 °C.

In conclusion, hierarchical morphologies, i.e., cylinders-in-lamella, lamellae-in-cylinder, and lamellae-in-sphere structures, have been found for the $I_{1.0}S_{1.8}P_X$ star-shaped terpolymers. The cylinders-in-lamella structures have smaller length-scale organizations of cylindrical structures, where the cylinders of the component I in lamellar matrix of S are oriented perpendicular to the lamellar planes, resulting in aligning normal to the film surface. In addition, the stacking manner of the hexagonal cylinder-arranged layers is identified to be random in the cylinders-in-lamella structure by SAXS measurement.

Acknowledgment. We thank Dr. J. Suzuki at the Center of Calculation in High Energy Accelerator Organization and Mr. J. Masuda at Nagoya University for their help in measuring small-angle X-ray scattering. This work was partially supported by a research grant from the 21st Century COE Program under support from the Japan Society for the Promotion of Science (JSPS) entitled "Nature-Guided Materials Processing" at the School of Engineering, Nagoya University. K.H. and Y.M. gratefully acknowledge the support under this grant. This work was also partly supported by a grant from PRESTO, Japan Science and Technology Corporation (JST), for which A.T. gratefully acknowledges the support.

References and Notes

(1) Muthukumar, M.; Ober, C. K.; Thomas, E. L. *Science* **1997**, *277*, 1225.
(2) Ruokolainen, J.; Mäkine, R.; Torkkeli, M.; Serimaa, R.; Mäkelä, T.; ten Brinke, G.; Ikkala, O. *Science* **1998**, *280*, 557.
(3) Ruokolainen, J.; ten Brinke, G.; Ikkala, O. *Adv. Mater.* **1999**, *11*, 777.
(4) Ikkala, O.; ten Brinke, G. *Science* **2002**, *295*, 2407.
(5) Nagata, Y.; Masuda, J.; Noro, A.; Cho, D.; Takano, A.; Y. Matsushita, *Macromolecules* **2005**, *38*, 10220.
(6) Masuda, J.; Takano, A.; Nagata, Y.; Noro, A.; Matsushita, Y. *Phys. Rev. Lett.* **2006**, *97*, 098301.
(7) Nap, R.; Kok, C.; ten Brinke, G.; Kuchanov, S. I. *Eur. Phys. J. E* **2001**, *4*, 515.
(8) Nap, R.; Erukhimovich, I. Y.; ten Brinke, G. *Macromolecules* **2004**, *37*, 4296.
(9) Nap, R.; Sushko, N.; Erukhimovich, I.; ten Brinke, G. *Macromolecules* **2006**, *39*, 6765.
(10) Li, Z.; Kesselman, E.; Talmon, Y.; Hillmyer, M. A.; Lodge, T. P. *Science* **2004**, *306*, 98.
(11) Li, Z.; Hillmyer, M. A.; Lodge, T. P. *Macromolecules* **2006**, *39*, 765.
(12) Hadjichristidis, N.; Iatrou, H.; Behal, S. K.; Chludzinski, J. J.; Disko, M. M.; Garner, R. T.; Liang, K. S.; Lohse, D. J.; Milner, S. T. *Macromolecules* **1993**, *26*, 5812.
(13) Okamoto, S.; Hasegawa, H.; Hashimoto, T.; Fujimoto, T.; Zhang, H.; Kazama, T.; Takano, A.; Isono, Y. *Polymer* **1997**, *38*, 5275.
(14) Sioula, S.; Hadjichristidis, N.; Thomas, E. L. *Macromolecules* **1998**, *31*, 5272.
(15) Sioula, S.; Hadjichristidis, N.; Thomas, E. L. *Macromolecules* **1998**, *31*, 8429.
(16) Hückstädt, H.; Göpfert, A.; Abetz, V. *Macromol. Chem. Phys.* **2000**, *201*, 296.
(17) Yamauchi, K.; Takahashi, K.; Hasegawa, H.; Iatrou, H.; Hadjichristidis, N.; Kaneko, T.; Nishikawa, Y.; Jinnai, H.; Matsui, T.; Nishioka, H.; Shimizu, M.; Furukawa, H. *Macromolecules* **2003**, *36*, 6962.
(18) Takano, A.; Wada, S.; Sato, S.; Araki, T.; Hirahara, K.; Kazama, T.; Kawahara, S.; Isono, Y.; Ohno, A.; Tanaka, N.; Matsushita, Y. *Macromolecules* **2004**, *37*, 9941.
(19) Abetz, V.; Jiang, S. *e-Polym.* **2004**, *no. 054*.
(20) Yamauchi, K.; Akasaka, S.; Hasegawa, H.; Iatrou, H.; Hadjichristidis, N. *Macromolecules* **2005**, *38*, 8022.
(21) Takano, A.; Kawashima, W.; Noro, A.; Isono, Y.; Tanaka, N.; Dotera, T.; Matsushita, Y. *J. Polym. Sci., Part B: Polym. Phys.* **2005**, *43*, 2427.
(22) Hayashida, K.; Kawashima, W.; Takano, A.; Shinohara, Y.; Amemiya, Y.; Nozue, Y.; Matsushita, Y. *Macromolecules* **2006**, *39*, 4869.
(23) Hayashida, K.; Takano, A.; Arai, S.; Shinohara, Y.; Amemiya, Y.; Matsushita, Y. *Macromolecules* **2006**, *39*, 9402.
(24) Bohbot-Raviv, Y.; Wang, Z.-G. *Phys. Rev. Lett.* **2000**, *85*, 3428.
(25) Gemma, T.; Hatano, A.; Dotera, T. *Macromolecules* **2002**, *35*, 3225.
(26) He, X.; Huang, L.; Liang, H.; Pan, C. *J. Chem. Phys.* **2002**, *116*, 10508.
(27) He, X.; Huang, L.; Liang, H.; Pan, C. *J. Chem. Phys.* **2003**, *118*, 9861.
(28) Tang, P.; Qiu, F.; Zhang, H.; Yang, Y. *J. Phys. Chem. B* **2004**, *108*, 8434.
(29) Lu, T.; He, X.; Liang, H. *J. Chem. Phys.* **2004**, *121*, 9702.
(30) Birshtein, T. M.; Polotsky, A. A.; Abetz, V. *Macromol. Theory Simul.* **2004**, *13*, 512.
(31) Dotera, T.; Gemma, T. *Philos. Mag.* **2006**, *86*, 1085.
(32) Takano, A.; Kawashima, W.; Wada, S.; Hayashida, K.; Sato, S.; Kawahara, S; Isono, Y.; Makihara, M.; Tanaka, N. Kawaguchi, D.; Matsushita, Y. to be submitted.
(33) Scattering intensities for a hexagonally-packed cylindrical structure where the volume fraction of the cylindrical domains is 0.35, are calculated as follows: 1 (100%), $\sqrt{3}$ (0.092%), 2 (4.52%), $\sqrt{7}$ (3.84%), and 3 (0.214%).
(34) Förster, S.; Khandpur, A. K.; Zhao, J.; Bates, F. S.; Hamley, I. W.; Ryan, A. J.; Bras, W. *Macromolecules* **1994**, *27*, 6922.
(35) Vigild, M. E.; Almdal, K.; Mortensen, K.; Hamley, I. W.; Fairclough, J. P. A.; Ryan, A. J. *Macromolecules* **1998**, *31*, 5702.
(36) Ahn, J.-H.; Zin, W.-C. *Macromolecules* **2000**, *33*, 641.
(37) Milner, S. T. *Macromolecules* **1994**, *27*, 2333.
(38) Matsushita, Y.; Watanabe, J.; Katano, F.; Yoshida, Y.; Noda, I. *Polymer* **1996**, *37* 321.
(39) Gunduz, S.; Dincer, S. *Polymer* **1980**, *21* 1041.

MA062972I